

Results show the robustness of the FDS scenario for pattern formation against the Turing scenario (for more details see paper [2]).

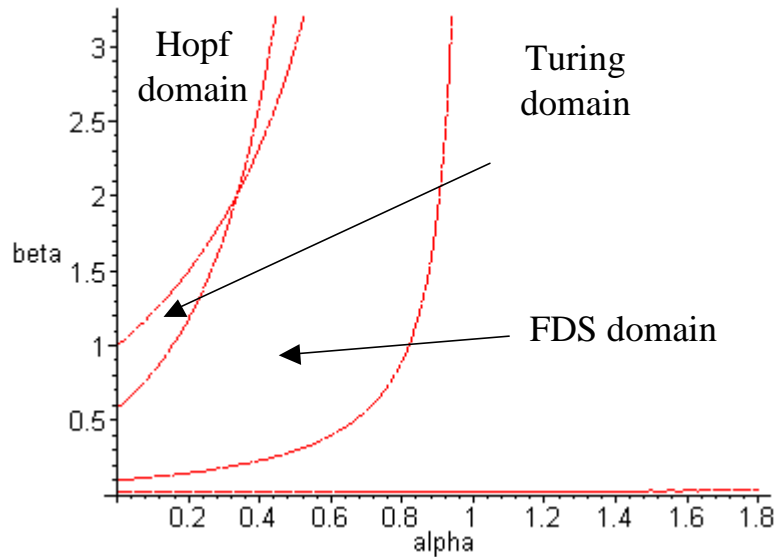


Figure 1. Typical spatial instability domains for the Gierer-Meinhardt model.

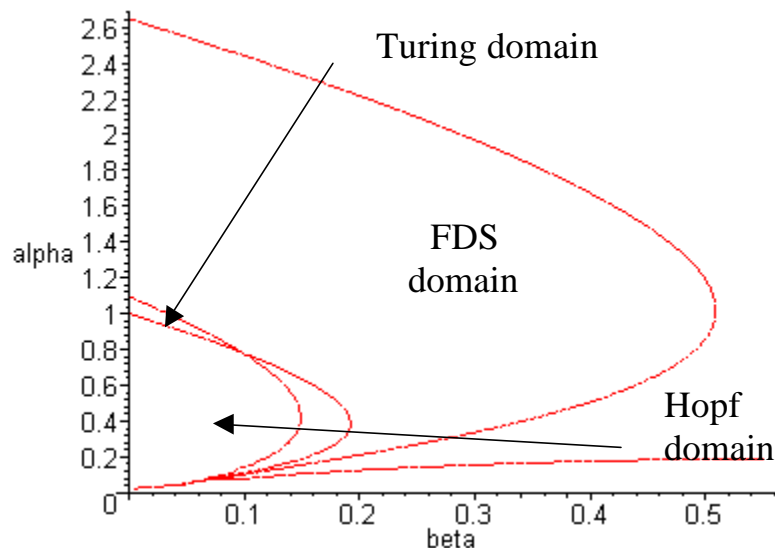


Figure 2. A typical plot of the spatial instability domains for the Schnakenberg kinetics.

In the above figures the axes labels represent controllable kinetics parameters. The two figures show that the FDS domain is much bigger than the Turing domain to which it always adjoins. In [2] it is explained how this and other features show that the Turing mechanism is just a particular and special case of a much larger and general pattern formation mechanism (FDS).

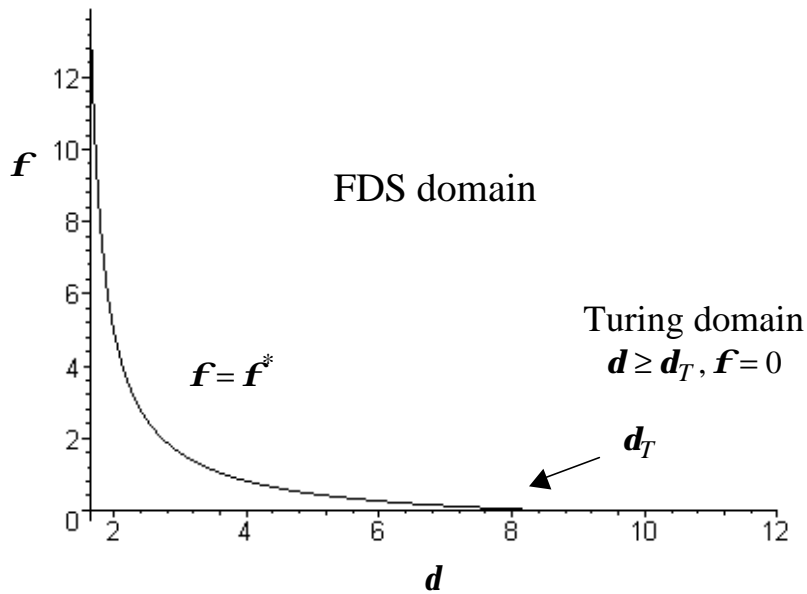


Figure 3 A plot in the (\mathbf{d}, \mathbf{f}) -plane of the generalised FDS domain for a generic cubic kinetics model. Turing critical diffusion is $\mathbf{d}_T \approx 8.39 > 1$. The pure Turing domain resides in the region $\mathbf{f} = 0, \mathbf{d} \geq \mathbf{d}_T$ along the \mathbf{d} -axes whereas the FDS domain lies in the whole domain bounded below by the curve $\mathbf{f} = \mathbf{f}^*$. Note the balance in the spatial transport needed to achieve spatial patterns: $\mathbf{f}^* \rightarrow \infty$ as \mathbf{d} becomes small and $\mathbf{f}^* \rightarrow 0$ as $\mathbf{d} \rightarrow \infty$ giving hyperbolae-shape behaviour.

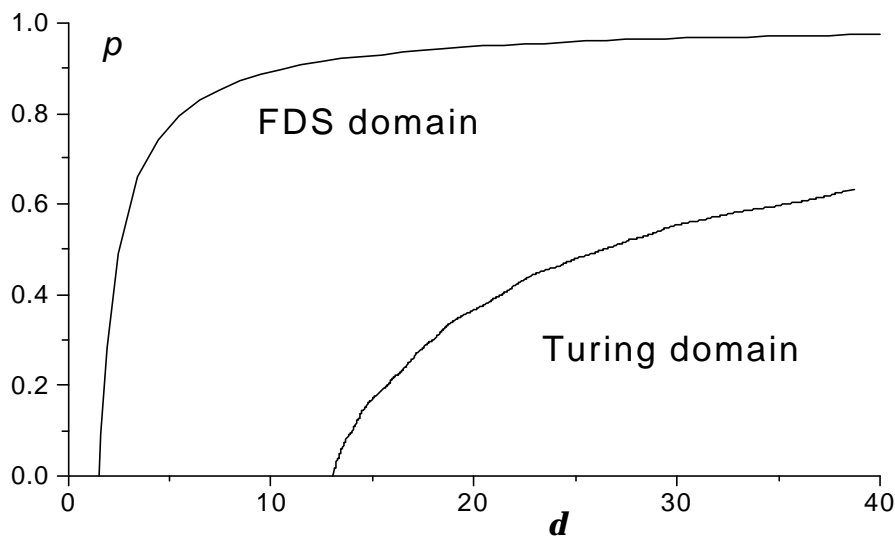


Figure 4. A plot of the boundaries for FDS and Turing domains in a generic cubic autocatalytic kinetics reaction-diffusion-advection system. p is the control kinetics parameter and \mathbf{d} is the ratio of the diffusion coefficients between the interacting species. It can be clearly seen the big improvement in the transport restrictions by diffusion in the FDS case against the Turing case. In the Turing case it is typical that the diffusion ratio is one order of magnitude (or more bigger) than 1. In the FDS case the ratio can be made as close to 1 as desired, which is very realistic for typical applications (in practice most morphogens have similar diffusion rates).

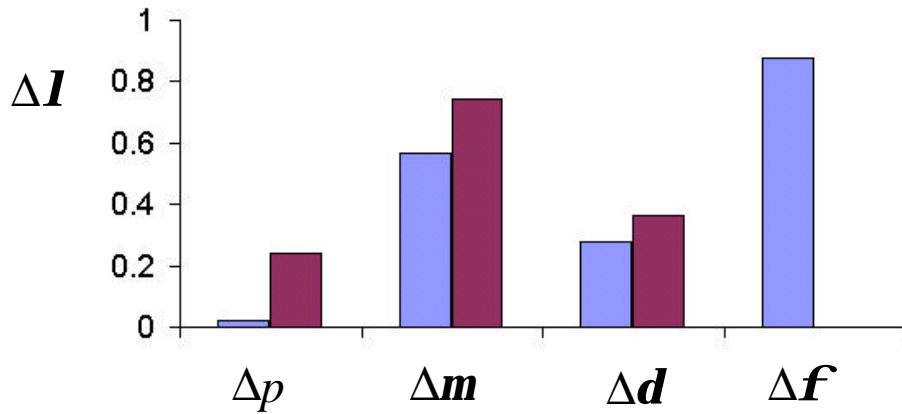


Figure 5. Results of the sensitivity analysis of the FDS and Turing patterns to parameter variations. This figure displays the percentage change in solution wavelength as function of $\pm 20\%$ percentage change in parameter values. The blue shading corresponds to FDS and magenta shading to the Turing cases respectively. Note that FDS solutions (i.e. when the advection rate $f > 0$) are more robust to parameter changes than the Turing solutions.

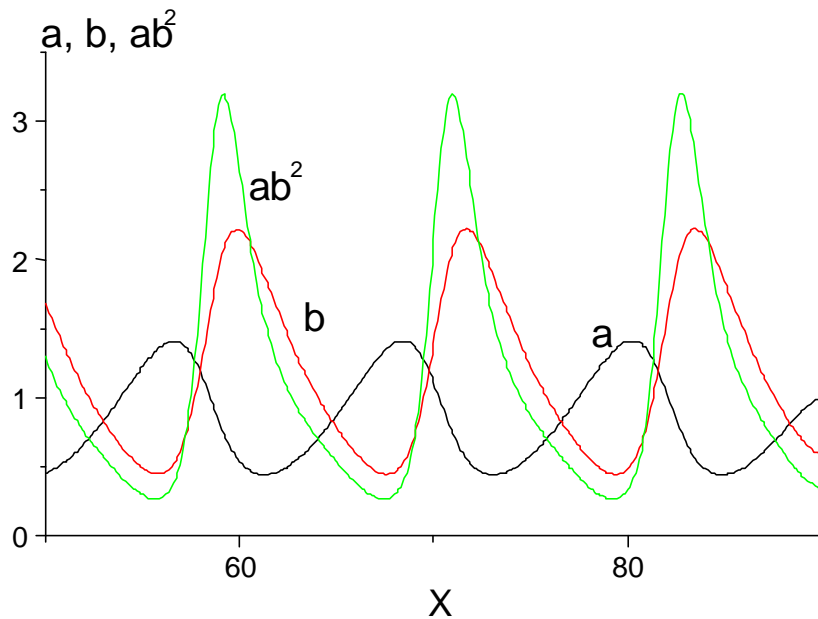


Figure 6. A typical plot for a FDS solution in a system of reaction-diffusion-advection system with cubic autocatalytic kinetics. The solutions are stationary. The black and red curves represent the concentrations of the substrate and respectively, the activator species and the green curve depicts the levels of the reaction rate. Note the phase shift between the peaks of the two species. This is a characteristic feature of dynamics in diffusion-advection systems.



Figure 7. Dimensionless concentrations for a generic cubic diffusion-advection system with cubic kinetics. Shown are FDS patterns with varying amplitude across the spatial domain.

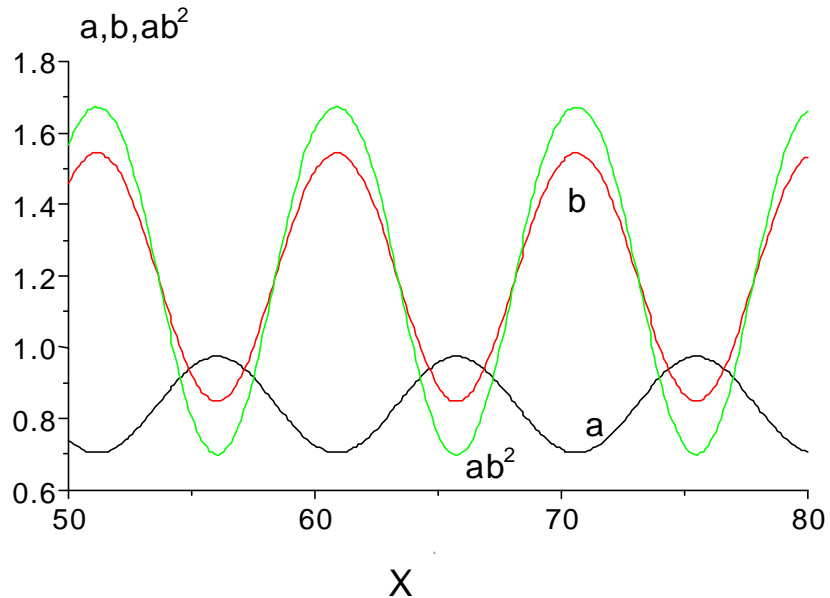


Figure 8. The same but with no advection present (Turing case). Note that the solutions are always out of phase (i.e. constant phase shift equal to π radians). Note also the considerable smaller concentrations attained with pure diffusion against the FDS case. All other conditions were the same in both simulations.